JOC Article
pubs.acs.org/joc

Effect of Electronegative Substituents and Angular Dependence on the Heteronuclear Spin−Spin Coupling Constant $^3J_{C-H}$: An Empirical Prediction Equation Derived by Density Functional Theory Calculations†

Giulia Palermo, Raffaele Riccio, and Giuseppe Bifulco*

Dipartimento di Scienze Farmaceutiche, University of Salerno, Via Ponte Don Melillo, 84084 Fisciano, Salerno, Italy

bifulco@unisa.it.

Received December 22, 2009

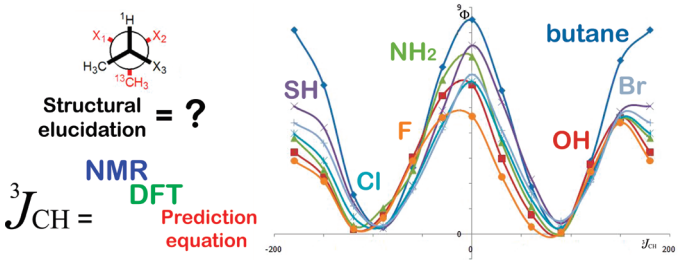

A general carbon−proton vicinal coupling constant ($^3J_{C-H}$) prediction equation has been empirically derived by a coupling constant database of 2157 $^3J_{C-H}$ calculations (at the hybrid DFT MPW1PW91/6-31G(d,p) level). The equation includes the electronegativity effect of the substituents attached to the $^{13}C-C-C-^1H$ fragment and the dihedral (Φ) dependence of the heteronuclear spin-coupling. A set of butane and pentane models were built, systematically varying both the Φ torsion angle in 30° steps and the substitution pattern with several electronegative substituents (Br, NH_2, F, Cl, SH, OH) in order to obtain the coupling constant database. The here reported $^3J_{C-H}$ equation is a quantitative prediction tool, particularly useful as a support in the analysis of NMR data for the structural elucidation of organic compounds characterized by specific substitution patterns. To confirm the accuracy of our equation in the prediction of the experimental $^3J_{C-H}$ couplings, we tested the equation, comparing 114 experimental $^3J_{C-H}$ values obtained from 29 polysubstituted benchmark organic compounds with the predicted data. In addition, a set of $^3J_{C-H}$ coupling bidimensional Karplus-type curves correlating the calculated $^3J_{C-H}$ values to the specific dihedral angle for every substitution pattern considered were built in order to evaluate the magnitude of the electronegativity effect.

Introduction

It is well-known that the ^3J homo- ($^1H-^1H$) and heteronuclear ($^1H-^{13}C$) NMR coupling constants play a key role in structural elucidation in many research areas. In fact, such parameters have been shown to be particularly useful in the stereostructural analysis of many organic compounds,[1] as witnessed by their extensive implication in many strategies approached by our and other research groups.[2] Furthermore, vicinal coupling constant ^3J analysis is becoming increasingly important in the study of the conformational properties of bioactive structures, for example, in the comprehension of the molecular basis of the interactions between small ligands and macromolecular targets.[3]

A number of appropriate NMR pulse sequences have long been used for the accurate reading of $^3J_{H-H}$ values;[4] more

† Dedicated to Prof. Saverio Florio on the occasion of his 70th birthday.

(1) Thomas, W. A. *Prog. Nucl. Magn. Reson. Spectrosc.* **1997**, *30*, 183–207.

(2) Bifulco, G.; Dambruoso, P.; Gomez-Paloma, L.; Riccio, R. *Chem. Rev.* **2007**, *107*, 3744–3779.

(3) (a) van Mourik, T.; Dingley, A. J. *Chem.—Eur. J.* **2005**, *11*, 6064–6079. (b) van Mourik, T.; Dingley, A. J. *ChemPhysChem.* **2007**, *8*, 288–296. (c) Erdélyi, M.; Pfeiffer, M.; Hauenstein, K.; Fohrer, J.; Gertsch, J.; Altmann, K. H.; Carlomagno, T. *J. Med. Chem.* **2008**, *51*, 1469–1473.

(4) (a) Hoye, R. T.; Hanson, P. R.; Vyvyan, J. R. *J. Org. Chem.* **1994**, *59*, 4096–4103. (b) Hoye, R. T.; Zhao, H. *J. Org. Chem.* **2002**, *67*, 4014–4016. (c) Biamonti, C.; Rios, C. B.; Lyons, B. A.; Montelione, G. T. *Adv. Biophys. Chem.* **1994**, *4*, 51–120.

Published on Web 02/25/2010 DOI: 10.1021/jo902704u

recently, modern NMR equipment and the introduction of the hetero half-filtered TOCSY (HETLOC)[5] and of other sequences (such as the HSQC-HECADE[6] and the phase-sensitive HMBC[7]) have gradually introduced heteronuclear long-range $^{2-3}J_{C-H}$ as complementary efficient tools for NMR structural elucidation of organic molecules. The correct interpretation of the NMR spectra for extrapolating the exact coupling constant values remains a fundamental issue, and in this regard, computational methods are a great support for NMR assignment; in particular, quantum mechanical (QM) calculations represent a powerful tool for both the interpretation and the prediction of experimental data.[2,8] The QM/NMR approach has been suggested as a quick and efficient method for the structural determination and/or revision of active natural compounds[2,9] and for the clarification of several medicinal and biological chemistry issues.[3] The state-of-the-art theory and the availability of new user-friendly quantum chemistry software packages represent a powerful combination for the straightforward comparison and prediction of experimental data, and particular efficiency has been shown in the prediction of spin−spin coupling constants.[10]

A widely used experimental approach for the determination of the relative configuration of organic compounds is the Murata method,[2,11] developed in the second half of the 1990s and based on $^{2,3}J$ qualitative patterns analysis. This approach has been successfully applied to many different compounds,[2,12] but it is based on the qualitative evaluation of the coupling constants, which are ranked in *small*/*large* $^{2,3}J$ patterns, and in controversial cases this qualitative method does not allow the clear discrimination between conformers. In addition, this approach does not take into account all variations of the dihedral angles, because it only considers staggered rotamers, and in case of two adjacent stereocenters bearing more than one electronegative substituent, $^{3}J_{C-H}$ analysis is not accurate for lack of specific reference patterns. All of these problems, together with the intrinsical narrow heteronuclear coupling constant range, are the major pitfalls in the *J*-based analysis, in particular in the case of acyclic organic compounds characterized by unusual substitution patterns on adjacent stereocenters. QM calculations may therefore be of support to the *J*-based analysis for the unambiguous determination of the relative configuration of atypical polysubstituded acyclic organic compounds, providing a quantitative comparison between experimental and predicted coupling constants but also complicating the analysis from the computational point of view.[3] Among others, Carreira et al. have recently proposed a detailed study enabling the configurational assignment of polychlorinated hydrocarbons named chlorosulfolipids through *J*-based analysis.[13] This study has highlighted once again the lack of a quantitative $^{3}J_{C-H}$ prediction tool for specifically polysubstituted compounds, even though the empirical quantitative prediction of the ^{3}J values has been the object of the development of several equations following the first Karplus model.[14] Such empirical equations may be an alternative to the use of quantum mechanical calculation methods for the accurate and fast prediction of ^{3}J couplings. In this paper we have undertaken a detailed study on the dependence of the heteronuclear vicinal coupling constant from both the dihedral angle between the nuclei in coupling (Φ) and the electronegativity of the substituents, with the aim to propose a new $^{3}J_{C-H}$ prediction equation including this parameters. Starting from a database of 2157 calculated (at the MPW1PW91[15]/6-31G(d,p) level) $^{3}J_{C-H}$ couplings, we derived a $^{3}J_{C-H}$ prediction equation (eq 7) that represents a general tool in the structural elucidation of polysubstituted organic compounds, providing a quantitative determination of the $^{3}J_{C-H}$ values associated with specific substitution patterns.

Homo- and Heteronuclear Coupling Constant Empirical Equations: Angular Dependence and Effect of Electronegative Substituents. The empirical derivation of the predicting ^{3}J equations is correlated to several factors: the intrinsic molecular features, the well-known dihedral angle (Φ) dependence extensively reported in literature,[16] and the effect of electronegative substituents attached to the $^{1}H-C-C-^{1}H$ or $^{13}C-C-C-^{1}H$ fragments.[17] In addition, previous studies have been complicated by the lack of sufficient experimental data regarding specific molecular fragments to be taken as a model in the empirical formulation of the equations. The most important equation including a relationship between the dihedral angle and the $^{3}J_{H-H}$ was developed by Karplus (eq 1),[14] and the Karplus curve was taken as starting point in the following studies regarding the vicinal coupling constants. The $^{1}H-^{1}H$ spin−spin relationship has been object of several attempts of reparameterization, focused on the

(5) (a) Kurz, M.; Schmieder, P.; Kessler, H. *Angew. Chem., Int. Ed. Engl.* **1991**, *30*, 1329–1331. (b) Wollborn, U.; Leibfritz, D. *J. Magn. Reson.* **1992**, *98*, 142–146.

(6) (a) Kozminski, W.; Nanz, D. *J. Magn. Reson.* **1997**, *124*, 383–392. (b) Kozminski, W.; Nanz, D. *J. Magn. Reson.* **2000**, *142*, 294–299.

(7) (a) Matsumori, N.; Murata, M.; Tachibana, K. *Tetrahedron* **1995**, *51*, 12229–12238. (b) Zhu, G.; Bax, A. *J. Magn. Reson.* **1993**, *104A*, 353–357. (c) Cicero, D. O.; Barbato, G.; Bazzo, R. *J. Magn. Reson.* **2001**, *148*, 209–213.

(8) (a) Chesnut, D. B. *Reviews in Computational Chemistry*; Lipkowitz, K. B., Boyd, D. E., Eds.; VCH Publishers: New York, 1996; Vol. 8. (b) Helgaker, T.; Jaszunski, M.; Ruud, K. *Chem. Rev.* **1999**, *99*, 293–352. (c) Fukui, H. *Prog. Nucl. Magn. Reson. Spectrosc.* **1999**, *35*, 267–294. (d) Contreras, R. H.; Peralta, J. E.; Giribet, C. G.; Ruiz de Azúa, M. C.; Facelli, J. C. *Annu. Rep. NMR Spectrosc.* **2000**, *41*, 55–184. (e) Bagno, A. *Chem.—Eur. J.* **2001**, *7*, 1652–1661.

(9) (a) Barone, G.; Gomez-Paloma, L.; Duca, D.; Silvestri, A.; Riccio, R.; Bifulco, G. *Chem.—Eur. J.* **2002**, *8*, 3233–3239. (b) Barone, G.; Duca, D.; Silvestri, A.; Gomez-Paloma, L.; Riccio, R.; Bifulco, G. *Chem.—Eur. J.* **2002**, *8*, 3240–3245. (c) Della Monica, C.; Randazzo, A.; Bifulco, G.; Cimino, P.; Aquino, M.; Izzo, I.; De Riccardis, F.; Gomez-Paloma, L. *Tetrahedron Lett.* **2002**, *43*, 5707–5710.

(10) (a) Alkorta, I.; Elguero, J. *Int. J. Mol. Sci.* **2003**, *4*, 64–92. (b) Contreras, R. H.; Barone, V.; Facelli, J. C.; Peralta, J. E. *Annu. Rep. NMR Spectrosc.* **2003**, *51*, 167–260. (c) Kaupp, M.; Buhl, M.; Malkin, V. G. *Calculation of NMR and EPR Parameters. Theory and Applications*; Wiley−VCH: Weinheim, 2004. (d) Bagno, A.; Rastrelli, F.; Saielli, G. *Chem.—Eur. J.* **2006**, *12*, 5514–5525. (e) Fukui, H. *Spec. Period. Rep. Nucl. Magn. Reson.* **2007**, *36*, 113–130. (f) Krivdin, L. B.; Contreras, R. H. *Annu. Rep. NMR Spectrosc.* **2007**, *61*, 133–245. (g) Vaara, J. *Phys. Chem. Chem. Phys.* **2007**, *9*, 5399–5418. (h) Bagno, A.; Saielli, G. *Theor. Chem. Acc.* **2007**, *117*, 603–619. (i) Helgaker, T.; Jaszunski, M.; Pecul, M. *Prog. Nucl. Magn. Reson. Spectrosc.* **2008**, *53*, 249–268. (j) Rastrelli, F.; Bagno, A. *Chem.—Eur. J.* **2009**, *15*, 7990–8004.

(11) (a) Matsumori, N.; Kaneno, D.; Murata, M.; Nakamura, H.; Tachibana, K. *J. Org. Chem.* **1999**, *64*, 866–876. (b) Sasaki, M.; Matsumori, N.; Maruyama, T.; Nonomura, T.; Murata, M.; Tachibana, K.; Yasumoto, T. *Angew. Chem., Int. Ed. Engl.* **1996**, *35*, 1672–1675.

(12) Bassarello, C.; Bifulco, G.; Evidente, A.; Riccio, R.; Gomez-Paloma, L. *Tetrahedron Lett.* **2001**, *42*, 8611–8613.

(13) Nilewski, C.; Geisser, W.; Ebert, M. O.; Carreira, E. M. *J. Am. Chem. Soc.* **2009**, *131*, 15866–15876.

(14) Karplus, M. *J. Chem. Phys.* **1959**, *30*, 11–15.

(15) Adamo, C.; Barone, V. *J. Chem. Phys.* **1998**, *108*, 664–675.

(16) Contreras, R. H.; Peralta, E. J. *Prog. Nucl. Magn. Reson. Spectrosc.* **2000**, *37*, 321–425.

(17) Glick, R. E.; Bothner-By, A. A. *J. Chem. Phys.* **1956**, *25*, 362–363.

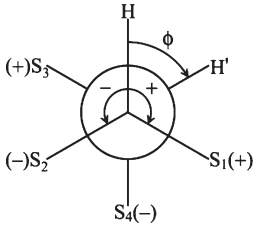

FIGURE 1. Altona's notation: "positive" (+) and "negative" (−) substituent positions with respect to the coupling protons.

introduction of specific terms describing the different systems under examination, such as nucleotides[18] or peptides.[19]

$$^3J_{H-H}(\Phi) = A + B\cos\Phi + C\cos(2\Phi) \quad (1)$$

As previously mentioned, the electronegativity (χ) of the substituents influences the coupling constant value, and in particular, it was shown that $^3J_{H-H}$ increases with the electronegativity as a function of the torsion angle Φ.[20] On the basis of this evidence, Abraham and Pachler[21] proposed eq 2, where $^3J_{H-H}$ values depend on coefficients (A−E), in turn linearly dependent on the electronegativity difference, $\Delta\chi = \chi_{subst} - \chi_{hydrogen}$.

$$^3J_{H-H}(\Phi) = A + B\cos\Phi + C\cos(2\Phi) + D\sin(\Phi) + E\sin(2\Phi) \quad (2)$$

Among the researchers interested in the empirical prediction of ^3J values, such as the Pachler[21] or Barfield groups,[22] a great contribution was given by Altona, who worked for a long time in the modification of the Karplus-type equation[23] and formulated eq 3, which takes into account both the substitution pattern and the dihedral angle.

$$^3J_{H-H}(\Phi) = P_1\cos^2\Phi + P_2\cos\Phi + P_3 + \sum\Delta\chi\,(P_4 + P_5\cos^2(\xi_i\Phi + P_6|\Delta\chi|)) \quad (3)$$

The parameters P_1-P_6 were empirically determined by a coupling constant data set derived from 315 models presenting a high variability of dihedral angles and substitution pattern, while ξ_i was associated to "positive" or "negative" substituents (equal to +1 or −1, respectively, depending on their positions; see Figure 1). The equation clearly highlights the $^3J_{H-H}$ dependence on both the torsion angle Φ and the substituent positions with respect to the coupling protons.

Subsequently, Díez et al. proposed new equations,[24] taking into account the interactions between substituents, and more recently, they published an interesting $^3J_{H-H}$ prediction study based on DFT calculations.[25]

Moreover, in the past years several user-friendly calculators based on the above equations have been developed for fast and straightforward coupling constant prediction.[26]

Concerning the $^3J_{C-H}$ coupling empirical prediction, many efforts were made starting from the Karplus equation, proposing specific prediction tools for peptides[27] and sugars[28] and leading to the development of the $^3J_{C-H}$ general Karplus-type equation (eq 4).[29] This equation was based on rigid adamantane or fenchane derivatives and did not contain any term regarding the electronegative effect of the substituents.

$$^3J_{C-H}(\Phi) = 4.5 - 0.78\cos\Phi + 4.03\cos(2\Phi) \quad (4)$$

Subsequent studies considered both the electronegativity and torsion angle factors, in particular taking into account the dihedral $^{13}C-C-C-^1H$ (Φ) and the dihedral angles ($\Psi_{\alpha,\beta,\gamma}$) between the substituents and the ^{13}C involved in the coupling ($X-^{13}C_\alpha-C_\beta-C_\gamma$, $X-C_\beta-C_\gamma-^1H$, $^{13}C_\alpha-C_\beta-C_\gamma-X$). Among the others, eq 5 was parametrized considering the 1-fluoropropane, showing the $^3J_{C-H}$ dependence on both the Φ_{C-H} and Ψ_{F-C} angles and introducing new C_n parameters associated with the two different angles.[30]

$$^3J_{C-H}(\Phi, \Psi_{F-C}) = C_{0,0} + C_{1,0}\cos\Phi + C_{2,0}\cos(2\Phi) + [C_{0,1} + C_{1,1}\cos\Phi + C_{2,1}\cos(2\Phi)]\cos\Psi \quad (5)$$

In the same paper, the authors extended this relationship to O, N, CH_3, and H α-propanes, building 340 models for the $^3J_{C-H}$ calculation and deriving a new specific equation for the α-substituited propanes (eq 6).

$$^3J_{C-H}(\Phi, \Psi_{X-C}) = (C_{00,0} + C_{01,0}\Delta\chi) + (C_{10,0} + C_{11,0}\Delta\chi)\cos\Phi + (C_{20,0} + C_{21,0}\Delta\chi)\cos(2\Phi) + \Delta\chi\cos\Psi\times[C_{01,1} + C_{11,1}\cos\Phi + C_{21,1}\cos(2\Phi)] \quad (6)$$

In a study regarding the conformational features of 12 iridoid glucosides, Morvai[31] successfully applied eq 6 in the $^3J_{C-H}$ prediction. In order to obtain calculated $^3J_{C-H}$ values in accordance with the experimental NMR data, he also had to consider β and γ substitution pattern effects, which are not described by the previous equation. Thus, starting from a study regarding the fluorine substituent effect in the α, β, and γ positions of monosubstituted propanes,[32] he derived an

(18) (a) Altona, C.; Sundaralingam, M. *J. Am. Chem. Soc.* **1973**, *95*, 2333–8212. (b) Davies, D. B.; Danyluk, S. S. *Biochemistry* **1974**, *13*, 4417–4434.
(19) Kopple, K. D.; Wiley, G. R.; Tauke, R. *Biopolymers* **1973**, *12*, 627–636.
(20) Abraham, R. J.; Gatti, G. *J. Chem. Soc. B* **1969**, 961–968.
(21) (a) Abraham, R. J.; Pachler, K. G. R. *Mol. Phys.* **1964**, *7*, 165–182. (b) Pachler, K. G. R. *Tetrahedron* **1971**, *27*, 187–199. (c) Pachler, K. G. R. *J. Chem. Soc., Perkin Trans.* **1972**, *2*, 1936–1940.
(22) (a) Barfield, M.; Smith, W. B. *J. Am. Chem. Soc.* **1992**, *114*, 1574–1581.
(23) (a) Haasnoot, C. A. G.; de Leeuw, F. A. A. M.; Altona, C. *Tetrahedron* **1980**, *36*, 2783–2792. (b) Haasnoot, C. A. G.; de Leeuw, F. A. A. M.; Altona, C. *Org. Magn. Reson.* **1981**, *15*, 43–52. (c) de Leeuw, F. A. A. M.; Altona., C.; Kessler, H.; Bernel, W.; Friedrich, A.; Krack, G.; Hull, W. E. *J. Am. Chem. Soc.* **1983**, *105*, 2237–2246. (d) Donders, L. A.; de Leeuw, F. A. A. M.; Altona, C. *Magn. Reson. Chem.* **1989**, *27*, 556–563. (e) Altona, C.; Ippel, J. H. W.; Hoekzema, A. J. A.; Erkelens, C.; Groesbeck, M.; Donders, L. A. *Magn. Reson. Chem.* **1989**, *27*, 564–576. (f) van Wijk, J.; Huckriede, B. D.; Ippel, J. H.; Altona, C. *Methods Enzymol.* **1992**, *2111*, 286–306. (g) Altona, C.; Franke, R.; de Haan, R.; Ippel, J. H.; Daalmans, G. I.; Hoekzema, W. A. J. A.; van Wijk, J. *Magn. Reson. Chem.* **1994**, *32*, 670–678.
(24) (a) Díez, E.; San-Fabián, J.; Guilleme, J.; Altona, C.; Donders, L. A. *Mol. Phys.* **1989**, *68*, 49–63. (b) Donders., L. A.; de Leeuw, F. A. A. M.; Altona, C. *Magn. Reson. Chem.* **1989**, *27*, 556–563.
(25) Díez, E.; Casanueva, J.; San-Fabián, J.; Esteban, A. L.; Galache, M. P.; Barone, V.; Peralta, H. E.; Contreras, R. H. *Mol. Phys.* **2005**, *103*, 1307–1326.
(26) (a) Navarro-Vázquez, A.; Cobas, J. C.; Sardina, F. J. *J. Chem. Inf. Comput. Sci.* **2004**, *44*, 1680–1685. (b) Balacco, G. *J. Chem. Inf. Comput. Sci.* **1996**, *36*, 885–887.
(27) Kao, L.-F.; Barfield, M. *J. Am. Chem. Soc.* **1985**, *107*, 2323–2330.
(28) Tvaroska, I.; Taravel, F. R. *Adv. Carbohydr. Chem. Biochem.* **1995**, *51*, 15–61.
(29) Aydin, R.; Günther, H. *Magn. Reson. Chem.* **1990**, *28*, 448–457.
(30) van Beuzekom, A. A.; de Leeuw, F. A. A. M.; Altona, C. *Magn. Reson. Chem.* **1990**, *28*, 68–74.
(31) Morvai, M.; Nagy, T.; Kocsis, A.; Szabó, F. S.; Podányi, B. *Magn. Reson. Chem.* **2000**, *38*, 343–359.
(32) San-Fabián, J.; Guilleme, J.; Díez, E. *J. Mol. Struct.* **1998**, *426*, 117–133.

approximate prediction parameter for refining the $^3J_{C-H}$ values. This parameter used in conjunction with eq 6 allowed him a correct $^3J_{C-H}$ analysis. Even though the prediction was confirmed by the analysis of the experimental data, the approach is based on an approximation not suitable for all organic molecules.

Many empirical deductions in the above coupling constant equations are derived from theoretical calculations, since a complete database of experimental ^3J values is not available. Moreover, considering that the ^3J theoretical calculation efforts increase for systems with complicated substitution patterns, the current equations for the $^3J_{C-H}$ prediction are based on simple and specific models. For this reason, the available $^3J_{C-H}$ prediction equations, even though somehow successfully applied, suffer for the lack of general applicability to complex organic molecules.

On the other hand, the researchers involved in the stereostructural determination would benefit from a rapid prediction tool allowing one to derive the $^3J_{C-H}$ values from parameters easy to spot. Furthermore, one of the major problems of the spectroscopists is the exact derivation of the conformational properties of the organic molecules and their stereochemical features; in both cases only a quantitative analysis could provide the exact angle between the two nuclei starting from the ^3J value.

In order to provide a 2-fold utility tool, allowing both the prediction of $^3J_{C-H}$ coupling constants and the derivation of the dihedral angle of interest (Φ), we propose here the new $^3J_{C-H}$ torsion angle based eq 7 including the electronegativity of the substituents for the accurate prediction of heteronuclear $^3J_{C-H}$ couplings

Results and Discussion

Taking as reference the Altona model with "positive" $S_i(+)$ and "negative" $S_i(-)$ substituents (Figure 1), we built a set of butane and pentane fragments, considering variations of 30° steps for the Φ torsion angle and systematically exploring the effect of the substitution pattern by inserting in the $S_i(+)$ and $S_i(-)$ positions the most common electronegative substituents of the organic molecules (Br, NH_2, F, Cl, SH, OH). Thus, we were able to evaluate the effect of the electronegative substituents in $S_i(\pm)$ for the β (carbon adjacent to the carbon involved in the coupling) and γ (carbon bearing the hydrogen involved in the coupling) positions, including these terms in the equation.

We named the original Altona $S_i(\pm)$ substituents on the hydrogen-bearing carbon H(+) and H(−) and the $S_i(\pm)$ substituents on the carbon involved in the coupling C(+) and C(−); such distinction is necessary because the symmetry of Altona's ^{1}H−C−C−^{1}H fragment is not present for our ^{13}C−C−C−^{1}H fragments. The choice of the models (Figure 2) favors a heterogeneous substitution pattern, with one and two substituents in the butane models and three substituents in the pentanes, allowing the calculation of 2157 $^3J_{C-H}$ couplings (all of the specific couplings are reported in Supporting Information).

We subjected these models to quantum chemical geometry optimization, fixing the dihedral angle of interest (Φ), at the DFT MPW1PW91/6-31G(d,p) level, and we performed on the obtained geometries the $^3J_{C-H}$ spin−spin coupling constant calculation at the same level of theory. To obtain the best reproducibility of the experimental NMR data, we chose the MPW1PW91/6-31G(d,p) level on the basis of previous works demonstrating its efficiency in the prediction of NMR parameters and in particular for the satisfactory results observed for the calculation of J values.[2,33−36] Moreover, the efficiency of such proton−proton and proton−carbon J coupling QM calculations has been used by our research group for the assignment of the relative configuration of complex organic molecules.[36,2] Besides all of the previous applications, the combination of the above functional and basis set has also been benchmarked on a large set of organic compounds; the results are reported in Supporting Information.

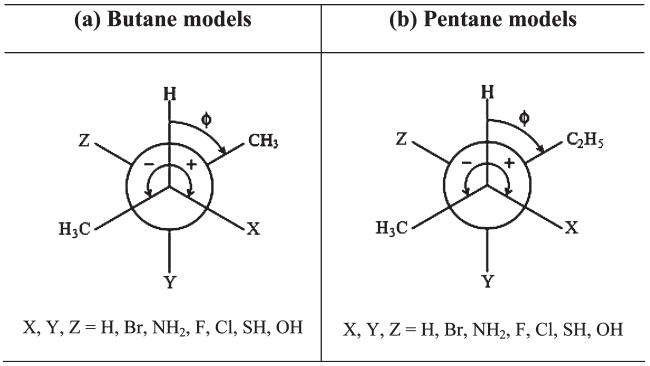

FIGURE 2. General pattern of the (a) butane and (b) pentane models. All 2157 models were built varying the Φ torsion angle in 30° steps and changing the substitution pattern in the $S_i(\pm)$ positions by permutation of the X, Y, and Z substituents.

Coupling Constant Torsion Angle Relationship for the Heteronuclear ^{1}H−^{13}C Spin−Spin Coupling Constant $^3J_{C-H}$. To extrapolate a new $^3J_{C-H}$ coupling constant equation including the electronegativity of the substituents, we started from the Altona $^3J_{H-H}$ equation (eq 3). This equation takes into account the electronegativity effect through the P_1-P_6 parameters, which were empirically determined on the basis of a database of 315 $^3J_{H-H}$ values. Starting from the Altona's prediction model and considering that the $^3J_{H-H}$ P_1-P_6 parameters are inappropriate for the description of the electronegativity effects on the three-bond heteronuclear coupling constant, we tried to empirically introduce new specific carbon−hydrogen P_n parameters. Furthermore, as stated above, in our model we have to deal with different electronegativity effects for the H($\pm$) γ-positions and the C($\pm$) β-positions, and therefore we propose here two different sets of P_n parameters: P_4, P_5, and P_6 associated to the H($\pm$) γ-effect and P_4', P_5', and P_6' parameters describing the C($\pm$) β-effect (Table 1).

$$^3J_{C-H}(\Phi) = P_1\cos^2\Phi + P_2\cos\Phi + P_3 + \sum\Delta\chi_{H(+/-)}(P_4 + P_5\cos^2(\xi_i\Phi + P_6|\Delta\chi_{H(+/-)}|)) + \sum\Delta\chi_{C(+/-)}(P_4' + P_5'\cos^2(\xi_i\Phi + P_6'|\Delta\chi_{C(+/-)}|)) \quad (7)$$

(33) Riccio, R.; Bifulco, G.; Cimino, P.; Bassarello, C.; Gomez-Paloma, L. *Pure Appl. Chem.* **2003**, *75*, 295–308.
(34) Cimino, P.; Gomez-Paloma, L.; Duca, D.; Riccio, R.; Bifulco, G. *Magn. Reson. Chem.* **2004**, *42*, S26–S33.
(35) Bassarello, C.; Cimino, P.; Gomez-Paloma, L.; Riccio, R.; Bifulco, G. *Tetrahedron* **2003**, *59*, 9555–9562.
(36) Bifulco, G.; Bassarello, C.; Riccio, R.; Gomez-Paloma, L. *Org. Lett.* **2004**, *6*, 1025–1028.

TABLE 1. P_n Parameters in Equation 7 Compared to the P_n Parameters in the Altona Equation (eq 3) and the A−C Parameters in the Karplus Equation (eq 1)

parameters	Karplus equation (eq 1)[14]	Altona equation (eq 3)[23a]	equation 7
A	7.76		
B	−1.1		
C	1.4		
P_1		13.36	8.40
P_2		−0.41	0.24
P_3		0	0
P_4		0.56	0.24
P_5		−2.32	−1.95
P_6		17.9	7.70
P_4'			0.38
P_5'			−1.49
P_6'			16.90

TABLE 2. Statistical Parameters for the $^3J_{C-H}$ Equation (eq 7) (rms-d and $\sum|\Delta J|/n$) Correlated to the Number of $^3J_{C-H}$ Coupling Calculations at the MPW1PW91/6-31G(d,p) Level for Every Set of Models Considered

models	no. of $^3J_{C-H}$ coupling calculations	rms-d[a]	$\sum\|\Delta J\|/n$[b]
butane models	1581	0.610	0.662
propane models	576	0.790	0.662
butane/propane models	2157	0.662	0.512

[a]rms-d = root mean square deviation (Hz) between the calculated (MPW1PW91/6-31G(d,p) level) $^3J_{C-H}$ coupling values and the values predicted by eq 7. [b]$\sum|\Delta J|/n = \sum|^3J_{C-H(G-03)} - {}^3J_{C-H(eq7)}|/n$ = average difference (Hz) between $^3J_{C-H}$ coupling constant values calculated at the MPW1PW91/6-31G(d,p) level and predicted through eq 7 in absolute value (n is the number of $^3J_{C-H}$ coupling calculations).

Our $^3J_{C-H}$ coupling equation includes all of the specific electronegativity terms on both atoms involved in the coupling; in particular the first three terms are correlated to the classical Karplus curve and to the relative trigonometric eq 1, while through the fourth and fifth terms, we have included the electronegativity effect of the $S_i(\pm)$ substituents with respect to both the ^1H and the ^{13}C involved in the coupling. The validity of our equation is confirmed by a series of statistical parameters, including the root mean square-deviation (rms-d), a good measure of the accuracy of our eq 7 in the reproduction of the calculated $^3J_{C-H}$ coupling values at the MPW1PW91/6-31G(d,p) level (Table 2). The comparison of our statistical data with Altona's homologue parameters concerning eq 3 for $^3J_{H-H}$ confirm the accuracy of eq 7 in the prediction of the $^3J_{C-H}$ coupling. Indeed, Altona and co-workers derived their equation by a 315 $^3J_{H-H}$ coupling set with an rms-d value of 0.541 Hz, whereas as previously noted the rms-d value related to our 2157 $^3J_{C-H}$ couplings is 0.662 Hz (Table 3). This difference is reduced if we consider only the butane models (1581 couplings), for which the rms-d value is 0.610 Hz (Table 2). An additional statistical parameter is the average difference between the $^3J_{C-H}$ coupling constant values calculated by MPW1PW91/6-31G(d,p) and those predicted by eq 7 in absolute value ($|\Delta J|/n$). Such value, reported in Table 2, is 0.512. The comparable rms-d values of the two equations represent a first proof of the efficiency of eq 7 in the prediction of the heteronuclear $^3J_{C-H}$ coupling constants of organic molecules.

In Table 3 we report the comparison between these statistical parameters and the same values calculated on our models. In Figure 3 are graphically reported the calculated $^3J_{C-H}$ couplings plotted versus those predicted by eq 7. The linear distribution of the $^3J_{C-H}$ values with respect to the average value is evident in the graph reported in Figure 3, showing good superposition between the calculated (at the MPW1PW91/6-31G(d,p) level) data and the couplings predicted by eq 7.

TABLE 3. Statistical Parameters for the $^3J_{H-H}$ Karplus Equation (eq 1), the $^3J_{H-H}$ Altona Equation (eq 3), and the $^3J_{C-H}$ Equation (eq 7), Obtained by Linear Fit of the Calculated (MPW1PW91/6-31G(d,p) Level) and Predicted Coupling Constant Values

statistical parameters	Karplus equation (eq 1)[14]	Altona equation (eq 3)[23a]	equation 7
rms-d[a]	1.201	0.541	0.662
slope	0.902	0.937	1.013
Intercept	0.607	0.003	−0.117
correlation coefficient (R^2)	0.947	0.991	0.889

[a]rms-d = root mean square deviation (Hz) between the calculated (MPW1PW91/6-31G(d,p) level) and $^3J_{C-H}$ coupling values predicted by eq 7.

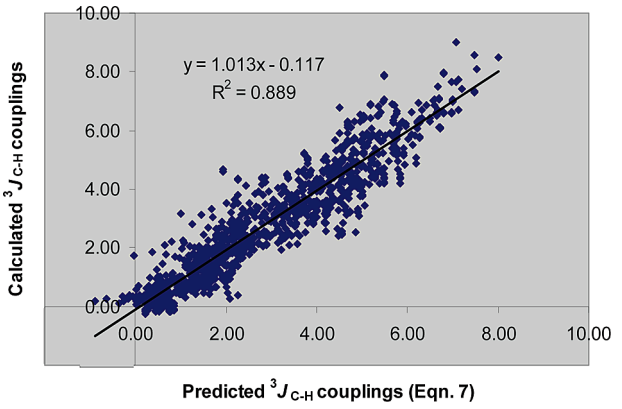

FIGURE 3. Calculated $^3J_{C-H}$ couplings (at the MPW1PW91/6-31g(d,p) level) plotted versus the values predicted by eq 7 for our butane and propane substituted models.

As previously said, one of the major problems in the elucidation of the relative configuration of organic molecules by J-based analysis is the exact derivation of the dihedral angle between the nuclei in the coupling.[11] In order to achieve a useful tool that allows one to directly connect the $^3J_{C-H}$ calculated values to the dihedral angle (Φ), we have also built a series of heteronuclear $^3J_{C-H}$ coupling bidimensional Karplus-type curves, starting from our calculated (at the MPW1PW91/6-31G(d,p) level) $^3J_{C-H}$ coupling database. Inspection of the Karplus-type curves allows one to directly observe the effect of the dihedral angle variation on the magnitude of the heteronuclear spin−spin coupling, in relation to the different specific substitution pattern. In Figure 4 are reported the superimpositions of the Karplus-type curves for some butane models as examples. We report the Karplus-type curves for all of the other substitution patterns in Supporting Information.

Reliability of Equation 7 in Reproduction of Experimental Heteronuclear $^3J_{C-H}$ Couplings. To confirm the accuracy of the prediction of the experimental $^3J_{C-H}$ couplings by our eq 7, we took as reference the following organic molecules (Chart 1): the potent antiviral marine peptide callipeltin

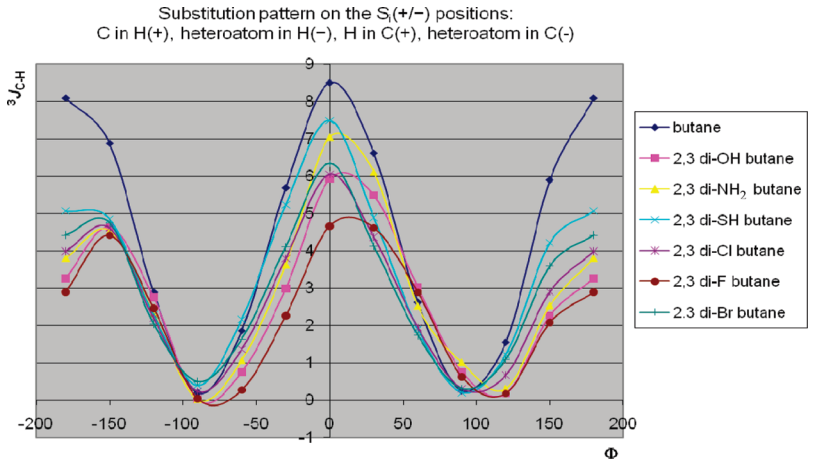

FIGURE 4. Superimpositions of the Karplus-type curves for the butane models characterized by the following substitution pattern in the S$_i$(±) positions: the heteroatom in the H(−) and the C(+) positions, the carbon atom in H(+) and the hydrogen atom in C(−). The heteronuclear $^3J_{C-H}$ couplings are plotted versus the dihedral angle between the nuclei in coupling (Φ), and the Karplus-type curves for the substituted models are related to the butane Karplus-type curve (in blue).

CHART 1. Potent Antiviral Marine Peptide Callipeltin A (1),[37] Polychlorinated Dipeptide Dysithiazolamide (2),[38] Ascaulitoxin Molecule (3),[12] Marine Natural Product Sphinxolide (4),[39] Marine Peptide Reidispongiolide A (5),[40] Depsipeptide Celebeside A (6),[41] and the Oxillipins (7, 8)[42]

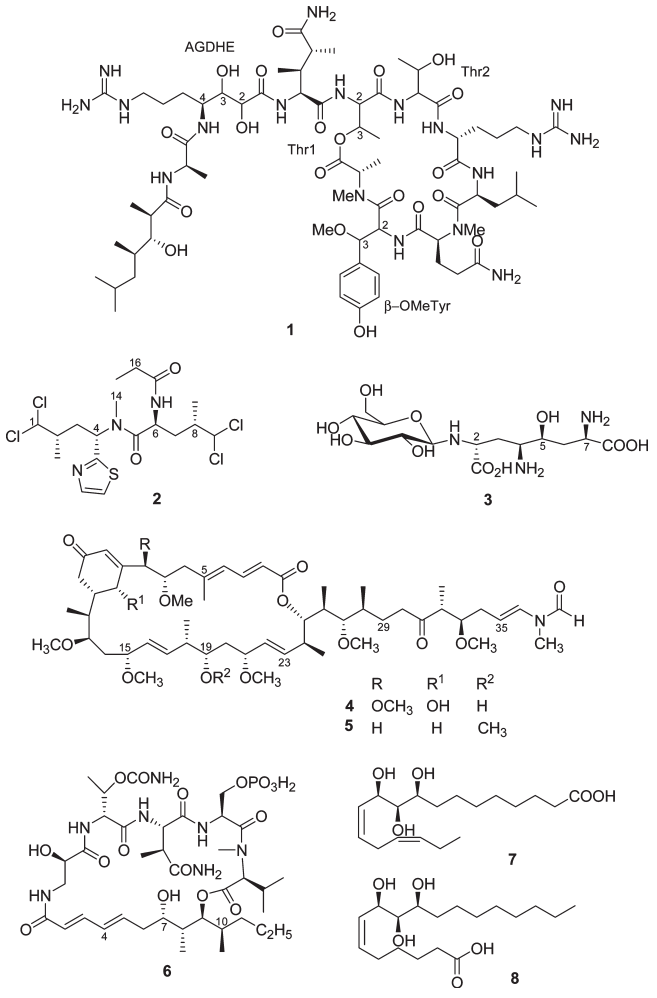

A (**1**),[37] the polychlorinated dipeptide dysithiazolamide (**2**),[38] the ascaulitoxin molecule (**3**),[12] the marine natural product sphinxolide (**4**),[39] the marine peptide reidispongiolide A (**5**),[40] the depsipeptide celebeside A (**6**),[41] and the oxillipins (**7** and **8**),[42] whose relative configurations were determined by theoretical and experimental studies. We chose these molecules as benchmarks because they well reproduce most of the problems associated with the structural determination of complex natural products. Indeed, they are not characterized by high structural rigidity, and the determination of the relative configuration by ^3J couplings was difficult. Also, we tried to mainly considered NMR experimental data collected from the HETLOC[5] NMR technique since it provides, when available, the most reliable and accurate reading of the $^3J_{C-H}$ values. By inspection of Table 4, reporting the experimental and predicted data for compounds **1**−**8**, it is noteworthy that there are mostly low error values in terms of average differences between the values predicted by eq 7 and the experimental data. This evidence is confirmed by an rms-d value of 0.859 Hz. The highest rms-d value reported for the benchmark compounds **1**−**8**, in comparison with the $^3J_{C-H}$ coupling data set taken as reference in the empirical derivation of our eq 7 (0.662 Hz, see Table 3), is referred to several factors, mainly the molecular structure of the natural products considered. The mobility of the chain, in fact, makes it difficult to identify the exact value of the dihedral angle between the nuclei in coupling (Φ), approximating the predicted $^3J_{C-H}$ coupling values through eq 7.

In addition to the experimental verification previously reported, we considered a series of rigid structures that provide a well determined set of torsion angles between the coupled nuclei. These benchmark structures are the methyl aldopyranosides **9**−**17** (Chart 2), having different configurations,

(37) Bassarello, C.; Zampella, A.; Monti, M. C.; Gomez-Paloma, L.; Auria, D; Riccio, M. V.; Bifulco, R. *Eur. J. Org. Chem.* **2006**, *3*, 604–609.
(38) Ardá, A.; Rodríguez, J.; Nieto, R. M.; Bassarello, C.; Gomez-Paloma, L.; Bifulco, G.; Jiménez, C. *Tetrahedron* **2005**, *61*, 10093–10098.
(39) Bassarello, C.; Bifulco, G.; Zampella, A.; D'Auria, M. V.; Riccio, R.; Gomez-Paloma, L. *Eur. J. Org. Chem.* **2001**, *1*, 39–44.
(40) Zampella, A.; Sepe, V.; D'Orsi, R.; Bifulco, G.; Bassarello, C.; D'Auria, M. V. *Tetrahedron: Asymmetry* **2003**, *14*, 1787–1798.
(41) Plaza, A.; Bifulco, G.; Keffer, J. L.; Lloyd, J. R.; Baker, H. L.; Bewley, C. A. *J. Org. Chem.* **2009**, *74*, 504–512.
(42) Benavides, A.; Napolitano, A.; Bassarello, C.; Carbone, V.; Gazzerro, P.; Malfitano, A. M.; Saggese, P.; Bifulco, M.; Piacente, S.; Pizza, C. *J. Nat. Prod.* **2009**, *72*, 813–817.

TABLE 4. Experimental $^3J_{C-H}$ Coupling Constant Values in Comparison with Those Predicted by Equation 7 for Natural Compounds 1−8, Differences between Predicted (eq 7) and Experimental $^3J_{C-H}$ Couplings in Absolute Value, $|\Delta^3J_{C-H}|$, and Average Difference in Absolute Value, $\sum|\Delta J|/n$

compound	label	dihedral angle[a] (Φ)	$^3J_{C-H(expt)}$[b]	$^3J_{C-H\ (eq\ 7)}$[c]	$\|\Delta^3J_{C-H}\|_{(eq\ 7-expt)}$[d]
1	H2−Me3 (Thr1)	180.00	5.00	4.73	0.27
1	H3−C═O (Thr1)	60.00	2.00	0.97	1.04
1	H2−C4 (AGDHE)	−60.00	2.60	2.67	0.07
1	H3−C═O (AGDHE)	60.00	1.20	2.64	1.44
1	H3−C5 (AGDHE)	−60.00	1.70	1.77	0.07
1	H4−C2 (AGDHE)	−60.00	1.20	1.23	0.03
1	H2−Ph (*β*-OMeTyr)	−60.00	1.30	2.55	1.25
1	H3−C═O (*β*-OMeTyr)	60.00	1.70	2.41	0.71
2	H6−C8	60.00	2.80	2.05	0.75
3	H5−C7	−60.00	2.10	2.14	0.04
3	H7−C5	−60.00	2.55	2.05	0.50
4	H32−C34	180.00	4.80	5.68	0.88
4	H33−C31	−60.00	0.50	1.28	0.78
4	H33−Me32	180.00	4.40	4.83	0.43
4	H28−C26	60.00	1.00	2.26	1.26
4	H27−C29	−60.00	2.20	2.19	0.01
4	H27−C28	60.00	1.40	1.38	0.02
4	H26−C28	60.00	0.50	1.21	0.71
4	H27−C25	180.00	6.70	4.83	1.87
4	H27−Me26	60.00	3.10	2.08	1.02
4	H26−C24	−60.00	0.50	1.21	0.71
4	H26−C27	−60.00	0.90	2.08	1.18
4	H25−Me26	180.00	6.70	4.83	1.87
4	H24−C26	−60.00	1.10	2.54	1.44
4	H25−Me24	180.00	1.40	1.38	0.02
5	H33−Me32	60.00	1.10	1.38	0.28
5	H27−C26	60.00	1.80	1.38	0.42
5	H26−C28	60.00	1.50	2.54	1.04
5	H24−C26	60.00	1.50	2.54	1.04
5	H25−Me24	60.00	1.40	1.38	0.02
5	H18−C20	60.00	1.00	2.54	1.54
5	H13−Me	−60.00	1.70	2.08	0.38
5	H11−Me12	−60.00	2.90	2.19	0.71
5	H11−C13	60.00	1.80	1.38	0.42
6	H9−Me8	60.00	1.30	1.38	0.08
7	H10−C12	−60.00	2.50	1.84	0.66
7	H9−C7	−60.00	2.30	1.84	0.46
8	H9−C11	60.00	1.90	1.32	0.59
8	H10−C8	60.00	1.90	1.32	0.59
$\sum\|\Delta J\|/n$[e]					0.682

[a] The dihedral angles (Φ) between the nuclei in coupling. [b] $^3J_{C-H\ (expt)}$ = experimental $^3J_{C-H}$ coupling constant values (Hz). [c] $^3J_{C-H\ (eq\ 7)} = {}^3J_{C-H}$ coupling constant values (Hz) predicted by eq 7. [d] $|\Delta^3J_{C-H}|_{(|eq\ 7-expt|)}$ = differences (Hz) between the predicted (eq 7) and the experimental $^3J_{C-H}$ couplings in absolute value. [e] $\sum|\Delta J|/n = \sum|^3J_{C-H(eq7)} - {}^3J_{C-H(expt)}|/n$ = average difference (Hz) value between the predicted (eq 7) and the experimental $^3J_{C-H}$ couplings in absolute value (n is the number of $^3J_{C-H}$ coupling calculations).

CHART 2. Methyl Aldopyranosides Synthesized by the Serianni Research Group[43]

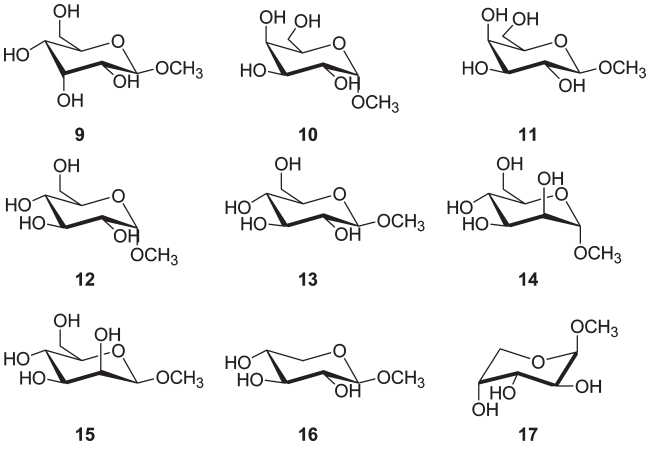

synthesized by the Serianni research group and characterized by selective ^{13}C-enrichment in order to derive the specific ring configurations by $^3J_{C-H}$ spin-coupling analysis.[43] Compounds **9**−**17** are methyl *β*-D-allopyranosyde **9**, methyl α-D-galactopyranosyde **10**, methyl *β*-D-galactopyranosyde **11**, methyl α-D-glucopyranosyde **12**, methyl *β*-D-glucopyranosyde **13**, methyl α-D-mannopyranosyde **14**, methyl *β*-D-mannopyranosyde **15**, methyl *β*-D-xylopyranosyde **16**, and methyl *β*-D-arabinopyranosyde **17.**

They are characterized by conformational stability that, besides the advantages already mentioned, permits a straightforward experimental NMR data interpretation. The torsion angles between C1 and H3 (Φ_{C1-H3}) derived from crystallographic studies are 66.2° for the aldopyranoside **11**,[44] 64.0° for **12**,[45] 65.5° for **13**,[46] 65.8° for **14**,[45] and 67.1° for **16**.[47] Regarding the Φ_{C2-H4}, crystallographic studies show a torsion angle (170.9°) for the methyl

(43) Podlasek, C. A.; Wu, J.; Stripe, W. A.; Bondo, P. B.; Serianni, A. S. *J. Am. Chem. Soc.* **1995**, *117*, 8635–8644.
(44) Takagi, S.; Jeffrey, G. A. *Acta Crystallogr.* **1979**, *B35*, 902–906.
(45) Jeffrey, G. A.; McMullan, R. K.; Takagi, S. *Acta Crystallogr.* **1977**, *B33*, 728–737.
(46) Jeffrey, G. A.; Takagi, S. *Acta Crystallogr.* **1977**, *B33*, 738–742.
(47) Takagi, S.; Jeffrey, G. A. *Acta Crystallogr.* **1977**, *B33*, 3033–3040.

TABLE 5. Experimental $^3J_{C-H}$ Coupling Constant Values in Comparison with Those Predicted by Equation 7 for Natural Compounds 9−17, Differences between Predicted (eq 7) and Experimental $^3J_{C-H}$ Couplings in Absolute Value, $|\Delta^3J_{C-H}|$, and Average Difference in Absolute Value, $\sum|\Delta J|/n$

compound	label	dihedral angle[a] (Φ)	$^3J_{C-H(expt)}$[b]	$^3J_{C-H(eq\ 7)}$[c]	$\|\Delta^3J_{C-H}\|_{(eq\ 7-expt)}$[d]
9	C3−H5	62.24	2.22	2.13	0.10
10	C2−H4	173.60	5.10	4.24	0.86
11	C1−H3	66.20	1.30	1.45	0.15
11	C2−H4	170.9	5.60	4.31	1.29
12	C3−H5	66.30	2.23	2.13	0.10
12	C4−H2	62.3	0.90	1.69	0.79
13	C1−H3	65.04	1.20	1.43	0.23
13	C3−H5	61.34	2.23	2.13	0.10
14	C1−H3	65.80	0.00	0.33	0.33
15	C3−H5	61.71	2.23	2.13	0.10
16	C1−H3	67.10	1.10	1.40	0.30
17	C2−H4	175.70	5.30	3.81	1.49
$\sum\|\Delta J\|/n$[e]					0.485

[a]The dihedral angles (Φ) between the nuclei in coupling. [b] $^3J_{C-H(expt)}$ = experimental $^3J_{C-H}$ coupling constant values (Hz). [c] $^3J_{C-H(eq\ 7)} = {}^3J_{C-H}$ coupling constant values (Hz) predicted by eq 7. [d] $|\Delta^3J_{C-H}|_{(eq\ 7-expt)}$ = differences (Hz) between the predicted (eq 7) and the experimental $^3J_{C-H}$ couplings in absolute value. [e] $\sum|\Delta J|/n = \sum|^3J_{C-H(eq\ 7)} - {}^3J_{C-H(expt)}|/n$ = average difference (Hz) value between the predicted (eq 7) and the experimental $^3J_{C-H}$ couplings in absolute value (n is the number of $^3J_{C-H}$ coupling calculations).

CHART 3. Chlorosulfolipid Structure Elucidated by Gerwick (18)[49] and Carreira's Polysubstituted Compounds (19−29)[13]

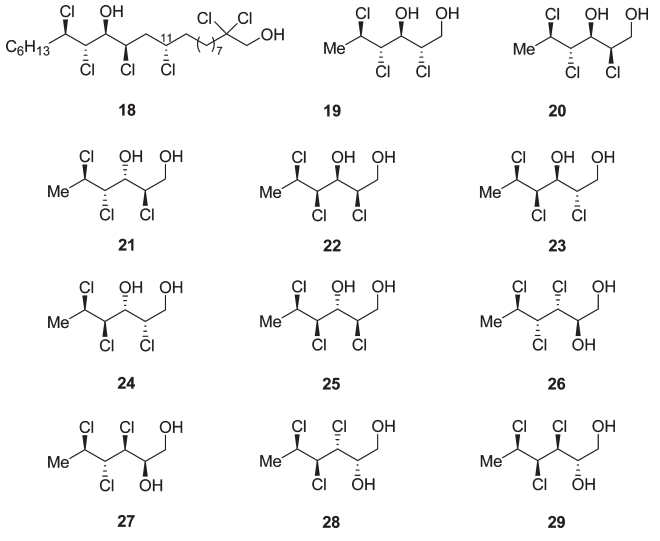

β-D-galactopyranosyde **11** smaller than that of the α anomer **10** (173.6°),[44] while for the methyl β-D-arabinopyranosyde **17** and the methyl α-D-galactopyranosyde **10**, the Φ_{C2-H4} angles are 175.7° and 173.6°, respectively.[44,48] For the Φ_{C3-H5} torsion angle, we took as reference the crystallographic value of 66.3° reported for the α-D-glucopyranosyde **12**,[45] while for the same structure the torsion angle between C4 and H2 (Φ_{C4-H2}) is 62.3°.[44] In Table 5 we report the experimental $^3J_{C-H}$ values and those predicted by eq 7 only for the X-ray determined torsion angles (Φ). In this case, the rms-d value is 0.681 Hz. Furthermore, we report an average absolute error between the predicted and experimental data $|\Delta J|/n$ of 0.485 Hz (Table 5).

Equation 7 is here proposed as a general prediction tool, useful in cases where other prediction methods are inadequate, such as in the case of polyalogenated compounds. For this reason, we took as reference a series of chlorosulfolipidic structures (see Chart 3) in our last benchmark run. The first of them is compound **18**, whose relative configuration was elucidated by the Gerwick research group in 2009,[49] and compounds **19**−**29** were synthesized by the Carreira research group in order to constitute a small coupling constant database for the specific *J*-based analysis of the polychlorinated compounds.[13]

In Table 6 is reported the comparison between the experimental $^3J_{C-H}$ coupling constant values and those predicted by eq 7. In this case the average absolute difference $|\Delta J|/n$ between the predicted and the experimental data is 0.677 Hz, and an rms-d value of 0.959 Hz is reported, confirming the efficiency of eq 7.

In Table 7 are reported the statistical parameters for all of the experimental 114 $^3J_{C-H}$ values (of the 29 benchmark organic compounds considered) and the respective values predicted through eq 7. As previously noted, the rms-d and the average differences $|\Delta J|/n$ values are a good measure of the accuracy of eq 7 in the reproduction of the experimental heteronuclear $^3J_{C-H}$ spin-couplings. Moreover, the signed average differences $\Delta J/n$, close to zero for all sets of compounds examined, suggests the absence of significant systematic errors associated with our equation. Even though the level of theory adopted for deriving the equation has been shown to provide high accuracy in the reproduction of $^3J_{C-H}$ values, the observed discrepancies between values predicted by eq 7 and experimental values could be due to the fact that our equation is purposely based only on the direct dependency on the dihedral angle and the electronegativity of adjacent substituents and does not take into account other effects (long-range, vibrational, solvent effects).

Conclusion

In this paper we propose a new $^3J_{C-H}$ coupling constant prediction equation (eq 7) including all of the specific electronegativity terms on both nuclei using nine P_n parameters, based on a coupling database of 2157 values obtained by DFT calculations at the MPW1PW91/6-31G(d,p) level. Low rms-d and average absolute difference ($|\Delta J|/n$) values demonstrate a satisfactory accuracy in the reproduction of the experimental NMR data for a large set of experimental

(48) Takagi, S.; Jeffrey, G. A. *Acta Crystallogr.* **1978**, *B34*, 1591–1596.

(49) Bedke, K. D.; Shibuya, G. M.; Pereira, A.; Gerwick, W. H.; Haines, T. H.; Vanderwal, C. D. *J. Am. Chem. Soc.* **2009**, *131*, 7570–7572.

TABLE 6. Experimental $^3J_{C-H}$ Coupling Constant Values in Comparison with Those Predicted by Equation 7 for Natural Compounds 18−29, Differences between Predicted (eq 7) and Experimental $^3J_{C-H}$ Couplings in Absolute Value, $|\Delta^3J_{C-H}|$, and Average Difference in Absolute Value, $\sum|\Delta J|/n$

compound	label	dihedral angle[a] (Φ)	$^3J_{C-H(expt)}$[b]	$^3J_{C-H(eq\ 7)}$[c]	$\|\Delta^3J_{C-H}\|_{(eq\ 7-expt)}$[d]
18	C10−H12a	60.00	2.70	2.55	0.15
18	C10−H12b	−60.00	1.50	1.63	0.13
18	H11−C13	−60.00	3.60	2.07	1.54
18	C14−H12a	−60.00	1.30	1.63	0.33
18	C14−H12b	60.00	0.80	2.43	1.63
18	C11−H13	−60.00	2.90	2.07	0.84
18	H13−C15	60.00	2.70	1.24	1.46
18	C12−H14	60.00	0.50	1.67	1.17
18	H14−C16	−60.00	0.50	2.59	2.09
18	C13−H15	60.00	2.00	2.57	0.57
18	H15−C17	180.00	7.80	4.73	3.07
18	C14−H16	−60.00	1.80	1.16	0.64
19	H2−C4	60.00	1.40	0.80	0.60
19	H4−C2	60.00	2.00	2.57	0.57
19	H4−C6	180.00	4.10	4.73	0.63
19	H5−C3	−60.00	1.50	1.16	0.34
20	H2−C4	−60.00	1.30	1.24	0.06
20	H4−C2	−60.00	3.10	2.57	0.53
20	H4−C6	180.00	4.60	4.73	0.13
20	H5−C3	60.00	1.80	1.16	0.64
21	H2−C4	60.00	2.00	2.57	0.57
21	H3−C1	−60.00	2.50	2.47	0.03
21	H3−C5	60.00	1.90	1.67	0.23
21	H4−C2	60.00	1.00	1.24	0.24
21	H4−C6	−60.00	2.30	2.40	0.10
21	H5−C3	60.00	2.40	2.40	0.00
22	H2−C4	60.00	1.60	1.24	0.36
22	H4−C2	60.00	1.70	2.13	0.43
22	H4−C6	60.00	1.90	1.60	0.30
22	H5−C3	60.00	1.30	1.60	0.30
23	H2−C4	60.00	2.10	2.57	0.47
23	H4−C2	60.00	1.40	1.24	0.16
23	H4−C6	60.00	2.80	1.96	0.84
23	H5−C3	60.00	3.20	1.96	1.24
24	H2−C4	−60.00	1.00	1.24	0.24
24	H3−C1	−60.00	2.00	1.67	0.33
24	H3−C5	60.00	1.90	2.47	0.57
24	H4−C2	−60.00	2.40	2.57	0.17
24	H4−C6	60.00	1.50	1.60	0.10
24	H5−C3	60.00	0.40	1.60	1.20
25	H2−C4	−60.00	1.10	0.80	0.30
25	H3−C1	180.00	3.90	4.20	0.30
25	H4−C2	−60.00	2.10	2.57	0.47
25	H4−C6	60.00	1.50	1.60	0.10
25	H5−C3	60.00	1.30	1.60	0.30
26	H3−C1	−60.00	3.10	2.57	0.53
26	H3−C5	60.00	0.00	1.60	1.60
26	H4−C2	60.00	1.40	1.60	0.20
26	H4−C6	180.00	2.50	4.73	2.23
26	H5−C3	180.00	2.30	4.73	2.43
27	H3−C1	60.00	1.60	2.57	0.97
27	H3−C5	−60.00	2.00	1.60	0.40
27	H4−C2	−60.00	2.60	1.60	1.00
27	H4−C6	60.00	4.50	2.40	2.10
27	H5−C3	−60.00	1.20	2.40	1.20
28	H4−C6	60.00	1.20	1.60	0.40
28	H5−C3	60.00	1.50	1.60	0.10
29	H2−C4	60.00	2.40	2.47	0.07
29	H3−C1	−60.00	2.60	2.57	0.03
29	H3−C5	60.00	3.60	1.60	2.00
29	H4−C2	60.00	1.20	1.60	0.40
29	H4−C6	60.00	1.90	1.96	0.06
29	H5−C3	60.00	1.50	1.96	0.46
$\sum\|\Delta J\|/n$[e]					0.677

[a] The dihedral angles (Φ) between the nuclei in coupling. [b] $^3J_{C-H(expt)}$ = experimental $^3J_{C-H}$ coupling constant values (Hz). [c] $^3J_{C-H(eq\ 7)} = {}^3J_{C-H}$ coupling constant values (Hz) predicted by eq 7. [d] $|\Delta^3J_{C-H}|_{(eq\ 7-expt)}$ = differences (Hz) between the predicted (eq 7) and the experimental $^3J_{C-H}$ couplings in absolute value. [e] $\sum|\Delta J|/n = \sum|{}^3J_{C-H(eq\ 7)} - {}^3J_{C-H(expt)}|/n$ = average difference (Hz) value between the predicted (eq 7) and the experimental $^3J_{C-H}$ couplings in absolute value (n is the number of $^3J_{C-H}$ coupling calculations).

$^3J_{C-H}$ spin-coupling values obtained from 29 benchmark organic compounds characterized by heterogeneous substitution patterns. In conclusion, eq 7 is an accurate and fast $^3J_{C-H}$ coupling prediction tool in the structural analysis of

TABLE 7. Statistical Parameters (RMS-d and $\sum\Delta J/n$) for Experimental $^3J_{C-H}$ Values and Those Predicted by Equation 7 for the 29 Benchmark Organic Compounds 1−29[a]

compounds	rms-d (eq 7−expt)[b]	$\sum\Delta^3J/n$ (eq 7−expt)[c]	$\sum\lvert\Delta^3J\rvert/n$ (eq 7−expt)[d]
1−8	0.859	0.106	0.682
9−17	0.681	−0.186	0.485
18−29	0.959	0.051	0.677
all[a]	0.900	0.045	0.658

[a]Statistical values for all 114 $^3J_{C-H}$ couplings considered. [b]rms-d = root mean square deviation (Hz) between experimental and predicted $^3J_{C-H}$ coupling values. [c]$\sum\Delta J/n$ = average difference (Hz) between $^3J_{C-H}$ coupling values prdicted by eq 7 and experimental values in relative value (n is the number of $^3J_{C-H}$ coupling calculations). [d]$\sum|\Delta J|/n$ = average difference (Hz) between $^3J_{C-H}$ coupling values predicted by eq 7 and experimental values in absolute value (n is the number of $^3J_{C-H}$ coupling calculations).

polysubstituted systems, straightforwardly providing, with known torsion angle between the atoms involved in the coupling and the substitution pattern on the $S_i(\pm)$ positions, the relative $^3J_{C-H}$ values.

Computational Details

All NMR $^3J_{C-H}$ coupling calculations were carried out using the Gaussian 03 Software Package,[50] with the hybrid DFT functional MPW1PW91 and the 6-31G(d,p) basis set. $^3J_{C-H}$ spin-coupling calculations were performed taking into account the contribution of the subsequent interactions: the most important Fermi contact (FC), paramagnetic spin−orbit (PSO), diamagnetic spin−orbit (DSO), and spin dipole (SD). All of the models under examination were subjected to a preliminary geometry optimization at the same level of theory, fixing the dihedral angle of interest (Φ) between the nuclei in the coupling. All calculation were performed on a four QuadXeon machine (16 CPUs). Electronegativities inserted in eq 7 are based on the Pauling electronegativity scale.[51]

Note Added after ASAP Publication. Equations 3 and 7 contained errors in the version published ASAP February 25, 2010; the correct version was posted to the web March 12, 2010.

Supporting Information Available: Calculated (at the MPW1PW91/6-31G(d,p) level) and predicted (through eq 7) $^3J_{C-H}$ coupling data for the 2157 butane and pentane models. Experimental and calculated (at the same MPW1PW91/6-31G(d,p) level of theory) $^3J_{C-H}$ couplings for the benchmark structures **1−29**. Superimpositions of the Karplus-type curves for the butane models characterized by different substitution patterns on the $S_i(\pm)$ positions. This material is available free of charge via the Internet at http://pubs.acs.org.

(50) Frisch, M. J.; Trucks, G. W.; Schlegel, H. B.; Scuseria, G. E.; Robb, M. A.; Cheeseman, J. R.; Montgomery, J. A., Jr.; Vreven, T.; Kudin, K. N.; Burant, J. C.; Millam, J. M.; Iyengar, S. S.; Tomasi, J.; Barone, V.; Mennucci, B.; Cossi, M.; Scalmani, G.; Rega, N.; Petersson, G. A.; Nakatsuji, H.; Hada, M.; Ehara, M.; Toyota, K.; Fukuda, R.; Hasegawa, J.; Ishida, M.; Nakajima, T.; Honda, Y.; Kitao, O.; Nakai, H.; Klene, M.; Li, X.; Knox, J. E.; Hratchian, H. P.; Cross, J. B.; Bakken, V.; Adamo, C.; Jaramillo, J.; Gomperts, R.; Stratmann, R. E.; Yazyev, O.; Austin, A. J.; Cammi, R.; Pomelli, C.; Ochterski, J. W.; Ayala, P. Y.; Morokuma, K.; Voth, G. A.; Salvador, P.; Dannenberg, J. J.; Zakrzewski, V. G.; Dapprich, S.; Daniels, A. D.; Strain, M. C.; Farkas, O.; Malick, D. K.; Rabuck, A. D.; Raghavachari, K.; Foresman, J. B.; Ortiz, J. V.; Cui, Q.; Baboul, A. G.; Clifford, S.; Cioslowski, J.; Stefanov, B. B.; Liu, G.; Liashenko, A.; Piskorz, P.; Komaromi, I.; Martin, R. L.; Fox, D. J.; Keith, T.; Al-Laham, M. A.; Peng, C. Y.; Nanayakkara, A.; Challacombe, M.; Gill, P. M. W.; Johnson, B.; Chen, W.; Wong, M. W.; Gonzalez, C.; Pople, J. A. *Gaussian 03*, Revision E.01; Gaussian: Wallingford, 2004.

(51) Pauling, L. *The Nature of Chemical Bond*, 3rd ed.; Cornell University Press: Ithaca, NY, 1960.